Robotica (2002) volume 20, pp. 395–404. © 2002 Cambridge University Press
DOI: 10.1017/S0263574702004162 Printed in the United Kingdom

An optimum robot path planning with payload constraints

Sezimaria F. P. Saramago* and Marco Ceccarelli†

(Received in Final Form: March 7, 2002)

SUMMARY
This paper presents a general methodology for the off-line planning of optimal trajectory of robot manipulators by taking into account the grasping forces in the manipulator gripper. The mechanical energy of the actuators has been considered for the formulation of the objective function. The optimization problem has been formulated as subject to physical constraints, input torque/force constraints and payload constraints. The mathematical model takes into account the coupled nonlinear equations of manipulator motion. A numerical example shows the efficiency of the proposed procedure.

KEYWORDS: Robotics; Programming; Path planning; Payload constraints.

1. INTRODUCTION

In many industrial applications the movements of the robot manipulators are planned manually in an *ad hoc* manner so that usually they do not perform the tasks with optimal paths. This path planning generally cannot be designed with the best paths or/and the maximum permissible speeds at all points along the programmed paths.

Repetitive processes are applied in robotic applications such as inspection, welding, painting, assembling, objects handling. The technological characteristic of these applications justifies off-line trajectory planning with optimum characteristics. When repetitive processes are imposed, it is possible to develop a methodology to move a robot manipulator along a specified optimum path. This can be achieved with minimum cost through an optimization problem formulation, in which an objective function can be defined by using the mechanical energy of the manipulator. For this purpose velocity and acceleration constraints can be considered together with force/torque and geometry constraints.

Considerable research has been done to obtain optimal robot path. But referring to the specific topic of this work, one can consider the following papers: Lin et al.[1] have proposed a procedure to construct a cubic polynomial joint trajectory and the algorithm for minimizing the traveling time subject to the physical constraints on joint velocities, accelerations and jerks. Shin and Mckay[2] have presented a solution to the problem of minimizing the cost of moving a robotic manipulator along a specified geometric path subject to input torque/force constraint, taking into account the dynamics of the manipulator. The method presented by Shiller and Dubowsky[3] has found the minimum time motion for a manipulator between given end states, by considering the full nonlinear manipulator's dynamics, actuator saturation characteristics, end-effector and payload constraints. Chen[4] has applied uniform cubic B-splines to solve the optimal trajectory planning problem for robotic manipulators subject to state and control constraints. Zeghloud and coauthors[5] have proposed an approach based on an optimization technique, which has consisted in determining a placement which minimizes an objective function describing the task. This work shows that many objective functions can be used in the placements problems and some of these functions consider only one criterion to be optimized. In the paper other multicriterion procedures have been considered for comparison with the proposed optimization. Chevallier and Payandeh[6] have proposed an approach for modelling and computing the grasping force as a function of the external forces (e.g. such as inertia actions), which can act on the grasped object. The contact between the fingers and object has been modelled as a point contact with friction. Zhao and Bai[7] have proposed optimal schemes, minimum load method, minimum torque method and multiple criterion method. In the last method, a weighted linear combination of joint torques and component loads is used as an objective function to formulate load distribution and joint trajectory planning. Johnson and Marsh[8] have described a model in which robot motions are represented using multivariate B-splines that have been used for collision avoidance and path planning. Park et al.[9] have presented a methodology for generating robot motions that are optimal with respect to physical criteria. Choi et al.[10] have discussed the problem of the minimum time trajectories and the control strategy to drive the robots along the trajectories when the exact dynamics equations of robots are unavailable. In each time interval the trajectory is optimized by means of the use of evolution strategy so that the total traveling time is minimized under the kinematic constraints. Arimoto[11] has edited a special issue of *Robotica* whose aim was to collect challenging research papers that reflect the state of the art of "grasping and manipulation" at the beginning of the new millennium.

In this paper, a general formulation has been proposed for optimum path planning of robot manipulators of an industrial type, taking into account the grasping forces in the manipulator gripper The proposed formulation has been deduced from separate experiences[12,13] of the authors also with the aim to combine the advantages of their previous approaches. The mechanical energy of the actuators is considered for the formulation of the objective function. The optimization problem has been formulated as subject to

* College of Mathematics, Federal University of Uberlandia, Uberlandia (MG) (Brazi); e-mail: saramago@ufu.br
† Laboratory of Robotics and Mechatronics – DiMSAT, University of Cassino, Via Di Biasio 43 – 03043 Cassino (Fr) (Italy); e-mail: ceccarelli@ing.unicas.it

https://doi.org/10.1017/S0263574702004162 Published online by Cambridge University Press

physical constraints, input torque/force constraints and payload constraints. The robot model has been based on the Denavit-Hartenberg parameters. A dynamical model for the manipulator has been obtained by writing the Euler-Lagrange's equation using the Lagrange's energy function in order to evaluate the mechanical energy of the actuator's action. Feasible trajectories have been defined using spline functions and then they have been obtained through off-line computation. A sequential technique has been used for the solving numerical optimization procedure. A numerical example involving a Puma 560 manipulator is presented to illustrate the numerical efficiency and feasibility of the proposed methodology.

2. A FORMULATION OF THE OPTIMUM PATH PLANNING

The path planning task for a manipulator with n degrees-of-freedom (d.o.f.) can be described using m knots for the trajectory for each i joint of the manipulator. The prescribed task can be given by the initial and final points P_0 and P_m of the trajectory, as shown in Figure 1, by taking into account additionally kinematic constraints and limits for the actuator forces and grasping force. The movement of the manipulator can be obtained by the simultaneous motion of the n joints in order to perform the prescribed task.

Among the many available criteria, one can assume the energy aspect as the most significant performance in order to optimize the manipulator operation, since the energy formulation can consider simultaneously dynamic and kinematic characteristics of the performing motion. Therefore, one can formulate the optimum path planning as an optimization problem in the form

$$\min E = \int_0^{t_m} \sum_{i=1}^{n} [\tau_i(t)\, \dot{q}_i(t)]^2 dt \tag{1}$$

Subject to

$$\begin{gathered} \max [q_i(t)] \le Q_i \\ \max [\dot{q}_i(t)] \le V_i \\ \max [\ddot{q}_i(t)] \le W_i \\ \max [\tau_i(t)] \le \Gamma_i \quad (i = 1, \ldots, n) \\ Fg_{min} \le F_k \le Fg_{max} \quad (k = 1, 2) \end{gathered} \tag{2}$$

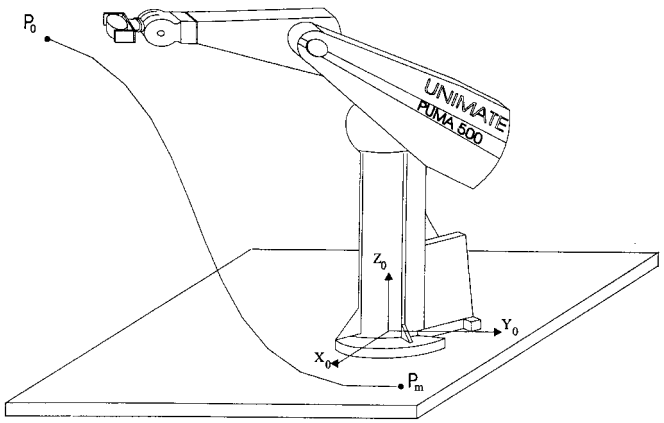


Fig. 1. A Puma 560 Robot Manipulator and a prescribed trajectory given by initial and final points.

where E is the total energy involved in the manipulator motion; τ_i is the actuator torque/force at joint i; q_i is the i-joint variable; t is the time variable in the interval $[0, t_m]$ for the path between P_o and P_m; the time derivatives of q_i are indicated as dot and double dot q_i; t_m is the prescribed time values at the end point P_m when $t=0$ is assumed at the initial point P_0 (Figure 1).

The constraints have been formulated in Equations (2) as functions of given limits for each i actuator in terms of maximum joint mobility Q_i, maximum velocity V_i, maximum acceleration W_i, and maximum torque Γ_i. In addition, payload constraints have been expressed in term of feasible range for the grasping forces F_1 and F_2 that ensure suitable static equilibrium of a grasping with two fingers.

The proposed formulation with Equations (1) and (2) requires the simultaneous computation and consideration of the manipulator dynamics and gripper statics.

3. KINEMATIC AND DYNAMIC MODEL OF A MANIPULATOR

Consider α_i, θ_i, d_i, a_i as the link Denavit-Hartenberg parameters for the robot manipulator. The homogeneous transformation matrix describing the relative translation and rotation between the link i coordinate system and the link $i-1$ coordinate system can be expressed as

$$T^i_{i-1} = \begin{bmatrix} \cos\theta_i & -\operatorname{sen}\theta_i \cos\alpha_i & \operatorname{sen}\theta_i \operatorname{sen}\alpha_i & a_i \cos\theta_i \\ \operatorname{sen}\theta_i & \cos\theta_i \cos\alpha_i & -\cos\theta_i \operatorname{sen}\alpha_i & a_i \operatorname{sen}\theta_i \\ 0 & \operatorname{sen}\alpha_i & \cos\alpha_i & d_i \\ 0 & 0 & 0 & 1 \end{bmatrix} \tag{3}$$

Thus, the kinematic motion of a robot manipulator with n d.o.fs. can be completely described by

$$T^n_o = T^1_0 T^2_1 T^3_2 \cdots T^n_{n-1} \tag{4}$$

Figure 2 represents the position vector r_i of a point in the i link as described with respect to link i. With respect to the base coordinates position vector r^i_o can be calculated as

$$r^i_o = T^i_o r_i = T^1_o T^2_1 \cdots T^i_{i-1} r_i \tag{5}$$

The corresponding velocity and acceleration of the point can be expressed as

$$\dot{r}_i = \left(\sum_{j=1}^{i} \left(\frac{\partial T^i_o}{\partial q_j} \dot{q}_j \right) \right) r_i \tag{6}$$

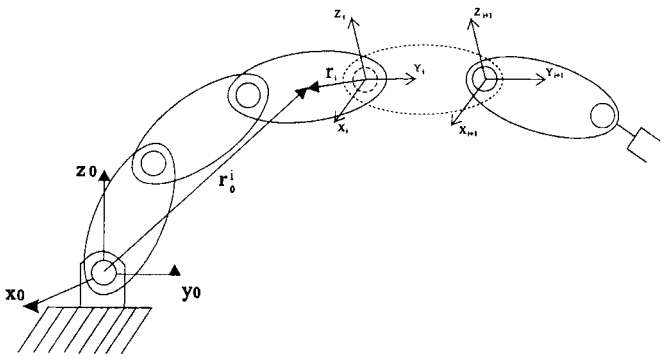


Fig. 2. The position vector r^i_o of a point on the i link.

https://doi.org/10.1017/S0263574702004162 Published online by Cambridge University Press

$$\ddot{r}_i = \left(\sum_{j=1}^{i} \left(\frac{\partial T_o^i}{\partial q_j} \ddot{q}_j \right) + \sum_{j=1}^{i} \left(\frac{\partial^2 T_o^i}{\partial q_j \partial q_k} \dot{q}_j \dot{q}_k \right) \right) r_i \qquad (7)$$

where

$$\frac{\partial T_{i-1}^i}{\partial q_i} = Df_i T_{i-1}^i \qquad (8)$$

in which, for rotational joints Df_i is given by

$$Df_i = \begin{bmatrix} 0 & -1 & 0 & 0 \\ 1 & 0 & 0 & 0 \\ 0 & 0 & 0 & 0 \\ 0 & 0 & 0 & 0 \end{bmatrix} \qquad (9)$$

and for prismatic joints Df_i is given by

$$Df_i = \begin{bmatrix} 0 & 0 & 0 & 0 \\ 0 & 0 & 0 & 0 \\ 0 & 0 & 0 & 1 \\ 0 & 0 & 0 & 0 \end{bmatrix} \qquad (10)$$

A simple notation, adopted by Saramago and Steffen,[14] can be used to write the derivative terms of the transformation matrix in a compact form as

$$U_{ij} = \frac{\partial T_o^i}{\partial q_j} = T_o^1 T_1^2 \cdots T_{j-2}^{j-1} (Df_j T_{j-1}^j) T_j^{j+1} \cdots T_{i-i}^i = T_o^{j-1} Df_j T_{j-1}^i \qquad (11)$$

and

$$U_{ijk} = \frac{\partial^2 T_o^i}{\partial q_k q_j} = \frac{\partial U_{ij}}{\partial q_k} = \begin{cases} T_o^{j-1} Df_j T_{j-1}^{k-1} Df_k T_{k-1}^i & \text{if} \quad j \le k \le i \\ T_o^{k-1} Df_k T_{k-1}^{j-1} Df_j T_{j-1}^i & \text{if} \quad k \le j \le i \\ 0 & \text{if} \quad j > i, \text{ or, } k > i \end{cases} \qquad (12)$$

Consequently, the expressions of Equations (6) and (7) can be rewritten as

$$\dot{r}_i = \left(\sum_{j=1}^{i} (U_{ij} \dot{q}_j) \right) r_i \qquad (13)$$

$$\ddot{r} = \left(\sum_{j=1}^{i} (U_{ij} \ddot{q}_j) + \sum_{j=1}^{i} (U_{ijk} \dot{q}_j \dot{q}_k) \right) r_i \qquad (14)$$

The dynamics of a robot manipulator can be modeled to compute the actuator forces/torques in the form

$$\tau = H(q)\ddot{q} + B(q)[\dot{q}\dot{q}] + C(q)[\dot{q}^2] + G(q) \qquad (15)$$

where

$$[\dot{q}\dot{q}] = [\dot{q}_1\dot{q}_2, \dot{q}_1\dot{q}_3, \ldots, \dot{q}_1\dot{q}_n, \dot{q}_2\dot{q}_3, \ldots, \dot{q}_2\dot{q}_n, \ldots, \dot{q}_{n-2}\dot{q}_n, \dot{q}_{n-1}\dot{q}_n]^T \; [\dot{q}^2] = [\dot{q}_1^2, \ldots, \dot{q}_{n-1}^2, q_n^2]^T \qquad (16)$$

in which τ is the vector of actuation torque/force, H(q) is the $n \times n$ kinetic energy matrix, B(q) is the $n \times n(n-1)/2$ matrix of Coriolis torques, C(q) is the $n \times n$ matrix of centrifugal torques, G(q) is the n-vector of gravity torques, q is the joint vector $q = [q_1, \ldots, q_n]^T$, where T is the transpose operator.

The dynamics simulation of a Puma 560 like manipulator can be carried out by using the formulation of Equations (15) and (16) in a numerical procedure like that proposed by Armstrong et al.[15]

The influence of the payload on the dynamic model of a robot can be considered by adding the grasped object mass to the mass of the last link. In the same way, the inertial moments of the given object can be added to the inertial moments of the last link through the expressions

$$m_n = m_{link}^n + m_{object} \qquad (17)$$

$$I_n = I_{link}^n + I_{object} \qquad (18)$$

4. A FORMULATION FOR TRAJECTORY MODELLING

In order to determine the joint trajectories, one can use the given initial and final points P_0 and P_m of Figure 1 in the Cartesian coordinates. These given points can be transformed into joint coordinates by solving the inverse kinematics. Then, cubic polynomial can be chosen to describe the joint trajectories since Proportional Derivative control is generally used for manipulator actuators in industrial robots.

Therefore, the trajectory $q_i(t)$ can be composed of uniform cubic B-splines with m knots at $0 = t_1 < t_2 < \ldots < t_{m-1} < t_m$ time coordinates to give

$$q_i(t) = \sum_{j=0}^{m-1} q_j^i(t), \quad i = 1, \cdots, n \qquad (19)$$

where the cubic B-spline can be expressed as

$$q_j^i(t) = \gamma_{j-3}^i \, b_{-3}(t) + \gamma_{j-2}^i \, b_{-2}(t) + \gamma_{j-1}^i \, b_{-1}(t) + \gamma_{j-0}^i \, b_{-0}(t) \qquad (20)$$

in which b_{-3}, b_{-2}, b_{-1}, b_{-0} are the basis function as formulated by Saramago and Steffen.[16] The coefficients γ_{j-3}^i, γ_{j-2}^i, γ_{j-1}^i, γ_{j-0}^i can be considered as unknowns for the optimal path planning and they can be computed by solving the linear system within the optimization problem as explained below.

The basis functions are non-zero over the time interval $[t_j, t_j + 4\delta]$ with $\delta = 1/(m-1)$; and they can be expressed as

$$b_{-0}(t, t_j) = \sigma_j^3(t)/6 \text{ and } \sigma_j(t) = \frac{(t - t_j)}{\delta} \text{ for } t \in [t_j, t_j + \delta]$$

$$b_{-1}(t, t_{j+1}) = [1 + 3\sigma_{j+1}(t) + 3\sigma_{j+1}^2(t) - 3\sigma_{j+1}^3(t)]/6 \text{ and}$$

$$\sigma_{j+1}(t) = \frac{(t - t_{j+1})}{\delta} \text{ for } t \in [t_{j+1}, t_{j+1} + \delta]$$

$$b_{-2}(t, t_{j+2}) = [4 - 6\sigma_{j+2}^2(t) + 3\sigma_{j+2}^3(t)]/6 \text{ and} \qquad (21)$$

$$\sigma_{j+2}(t) = \frac{(t - t_{j+2})}{\delta} \text{ for } t \in [t_{j+2}, t_{j+2} + \delta]$$

$$b_{-3}(t, t_{j+3}) = [1 - 3\sigma_{j+3}(t) + 3\sigma_{j+3}^2(t) - \sigma_{j+3}^3(t)]/6 \text{ and}$$

$$\sigma_{j+3}(t) = \frac{(t - t_{j+3})}{\delta} \text{ for } t \in [t_{j+3}, t_{j+3} + \delta]$$

https://doi.org/10.1017/S0263574702004162 Published online by Cambridge University Press

Since $q_j^i(t)$ is a cubic, its derivatives with respect to t can be straightforwardly computed as

$$\frac{d^k q_j^i(t)}{dt^k} = \gamma_{j-3}^i b_{-3}^{(k)}(t) + \gamma_{j-2}^i b_{-2}^{(k)}(t) + \gamma_{j-1}^i b_{-1}^{(k)}(t) + \gamma_{j-0}^i b_{-0}^{(k)}(t) \tag{22}$$

where

$$b_{-j}^{(k)} = \frac{d^k(b_{-j})}{dt^k} \tag{23}$$

The initial guess for the unknown coefficients of the B-splines can be obtained by fitting a straight line joining the given initial value q_0^i and final value q_m^i $(i=1, \ldots, n)$ for each joint.

When the m points and terminal time t_m are given, Equation (19) is a function of the n(m+2) unknowns γ_j^i $(i=1, \ldots, n;\ j=1, \ldots, m)$. The number of equations for each joint is m. Thus, using Equation (22) and the given initial and final velocities for each joint, two new equations can be added to the linear system to obtain

$$\begin{aligned} &D[\gamma_{-3}^i\ \gamma_{-2}^i\ \gamma_{-0}^i\ \gamma_{-1}^i\ \cdots\ \gamma_{m-1}^i\ \gamma_m^i]^T \\ &= [q_0^i\ q_2^i\ q_3^i\ \cdots\ q_m^i\ \dot{q}_0^i\ \dot{q}_m^i]^T \quad i=1, \ldots, n \end{aligned} \tag{24}$$

in which the entries of matrix D can be calculated using the basis functions given by Equation (21). Thus, entries of matrix D, with index k varying from 1 to m and index j varying from 1 to m − 1, can be computed as

$$\begin{aligned} D(k, j) &= D(k, j) + b_{-3} \\ D(k, j+1) &= D(k, j+1) + b_{-2} \\ D(k, j+2) &= D(k, j+2) + b_{-1} \\ D(k, j+3) &= D(k, j+3) + b_{-0} \end{aligned} \tag{25}$$

in which

$$\begin{aligned} b_{-0} &= \sigma^3/6 \\ b_{-1} &= (1 + 3\sigma + 3\sigma^2 - 3\sigma^3)/6 \\ b_{-2} &= (4 - 6\sigma^2 + 3\sigma^3)/6 \\ b_{-3} &= (1 - 3\sigma + 3\sigma^2 - \sigma^3)/6 \end{aligned} \tag{26}$$

with

$$\sigma = (t(k) - t(j))/\delta \quad \text{for} \quad t(k) > t(j) \tag{27}$$

and

$$\sigma = 0 \quad \text{for} \quad t(k) \le t(j) \tag{28}$$

The entries of the two last lines of matrix D can be calculated using Equation (22) with the index k varying from 1 to 2 and index j varying from 1 to m − 1, in the form

$$\begin{aligned} D(k+m, j) &= D(k+m, j) + \dot{b}_{-3} \\ D(k+m, j+1) &= D(k+m, j+1) + \dot{b}_{-2} \\ D(k+m, j+2) &= D(k+m, j+2) + \dot{b}_{-1} \\ D(k+m, j+3) &= D(k+m, j+3) + \dot{b}_{-0} \end{aligned} \tag{29}$$

in which

$$\begin{aligned} \dot{b}_{-0} &= \sigma^2/(2\delta) \\ \dot{b}_{-1} &= (1 + 2\sigma - 3\sigma^2/(2\delta) \\ \dot{b}_{-2} &= (-4\sigma + 3\sigma^2/(2\delta) \\ \dot{b}_{-3} &= (-1 + 2\sigma - \sigma^2/(2\delta) \end{aligned} \tag{30}$$

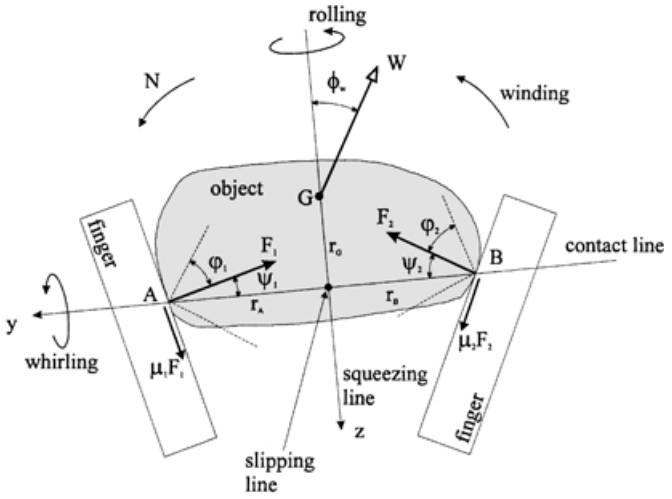


Fig. 3. Configuration and forces for a planar grasp with two fingers.

Table I. Denavit-Hartenberg Parameters for the Puma 560.[15,19]

Link	θ_i (degree)	α_i (degree)	a_i (m)	d_i (m)
1	q_1	–90	0	0
2	q_2	0	0.4318	0
3	q_3	–90	0.0203	0.1254
4	q_4	90	0	0.4318
5	q_5	–90	0	0
6	q_6	0	0	0

Table II. Mass (Kg), center of mass (m), Inertia dyadics and effective motor inertia (Kg/m^2) for the Puma 560 as deduced from references [15], [19].

Link	M_i	r_x	r_y	r_z	I_{xx}	I_{yy}	I_{zz}	I_m
1	–	–	–	–	0	0	0.350	1.140
2	18.50	0.068	0.006	–0.016	0.130	0.5240	0.539	4.710
3	4.80	0	–0.070	0.014	0.066	0.0125	0.086	0.830
4	0.94	0	0	–0.019	1.80×10^{-3}	$1.80\times10-3$	$1.30\times10-3$	0.200
5	0.54	0	0	0	0.30×10^{-3}	0.30×10^{-3}	0.40×10^{-3}	0.179
6	0.10	0	0	0.032	0.15×10^{-3}	0.15×10^{-3}	0.04×10^{-3}	0.193

https://doi.org/10.1017/S0263574702004162 Published online by Cambridge University Press

with

$$\sigma = \{t[(k-1)m] - t(j)\}/\delta \quad \text{for} \quad t[(k-1)m] > t(j) \quad (31)$$

and

$$\sigma = 0 \quad \text{for} \quad t[(k-1)m] \leq t(j) \quad (32)$$

Thus, a trajectory for a joint variable q_i can be determined when Equation (20) is numerically computed by using Equations (21) to (32).

5. A FORMULATION OF THE GRASPING FORCES IN THE GRIPPER

Usually, industrial robots use two-finger grippers for grasping purposes. In Figure 3, F_1 and F_2 are the grasping forces, which are exerted by the fingers and usually they are not equal, since the contact points A and B (which are assumed as application points for the forces) are not generally located in the same relative position on the two fingers.[17] A similar observation can be developed for the friction evaluation at the points A and B through the coefficients μ_1 and μ_2. The angles of the friction cones are φ_1 and φ_2. The grasping configuration of the object with respect to the fingers gives the angles ψ_1 and ψ_2, which strongly depend on the orientation of the fingers, the position of the contact points, the shape of the object and the fingers. These angles can differ from each other. However, because of the symmetry of a two-finger gripper, in a simulation procedure, it is convenient to assume them as equal to the most unfavourable value, which refers to the case that gives a squeezing component from the grasping force itself. The grasping forces can exert this pushing action yet through the component F sin ψ.

In Figure 3 the planar grasp by two fingers has been modelled by using the above mentioned considerations.[17,18] In addition r_A and r_B represent the distances of A and B, respectively, from the squeezing line. The distance of the gravity centre of the grasped object is indicated as r_G. $W = m_{object}\ g$ is the weight vector of the object and it is oriented with an angle Φ_W with respect to the squeezing line and an angle ψ_W with respect to the perpendicular axis to the plane yz. N is an external torque acting on the object and it includes the inertial actions due to the manipulator movement. This model can describe all the situations, which may

Table III. Constraints for Puma Robot as deduced from the data in reference [19].

Constraint	1	2	3	4	5	6
Q_i (degrees)	320	250	270	280	200	532
V_i (degrees/sec)	82	74	122	228	241	228
W_i (degrees/sec^2)	286	286	572	572	572	572
Γ_i (Nm)	77	133	66	13	12	13

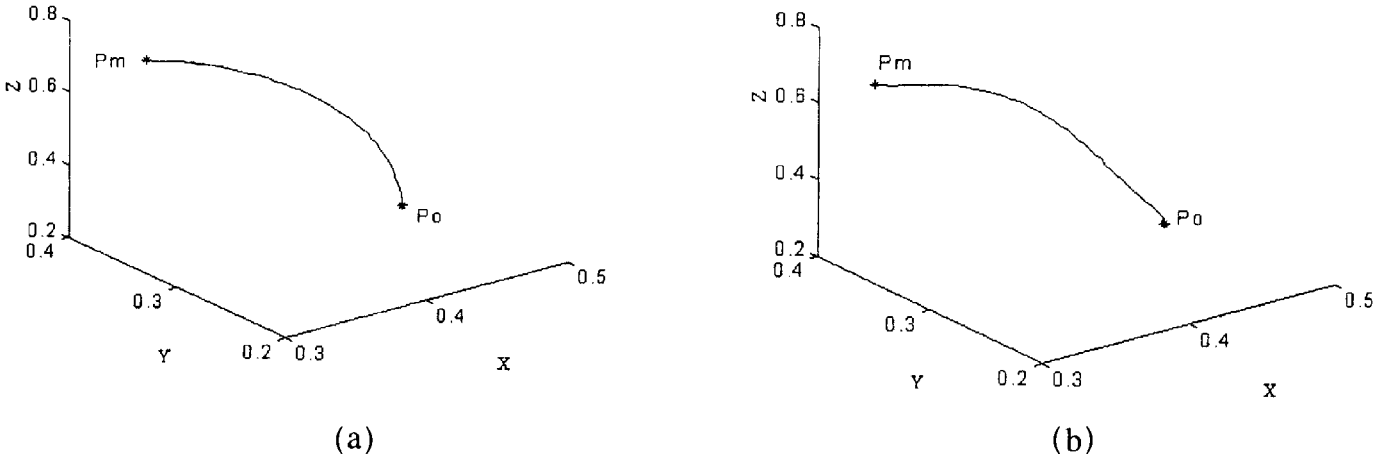


Fig. 4. An illustrative numerical example of optimum path planning for a Puma Robot with data of Tables I, II, and III: (a) the given points P_0 and P_m with the initial guess path; (b) the designed optimum path. (Coordinates are expressed in meters units.)

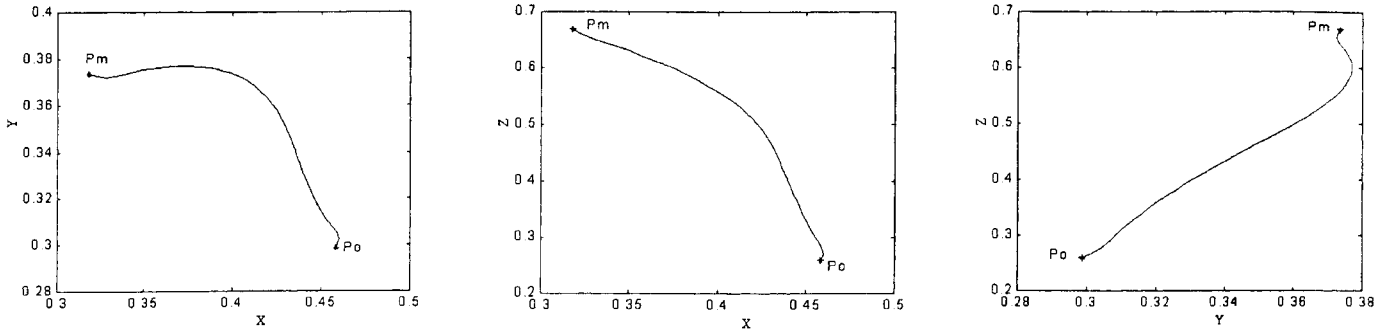


Fig. 5. Cartesian projections of the designed optimum path of Fig. 4b. (Coordinates are expressed in meters units.)

https://doi.org/10.1017/S0263574702004162 Published online by Cambridge University Press

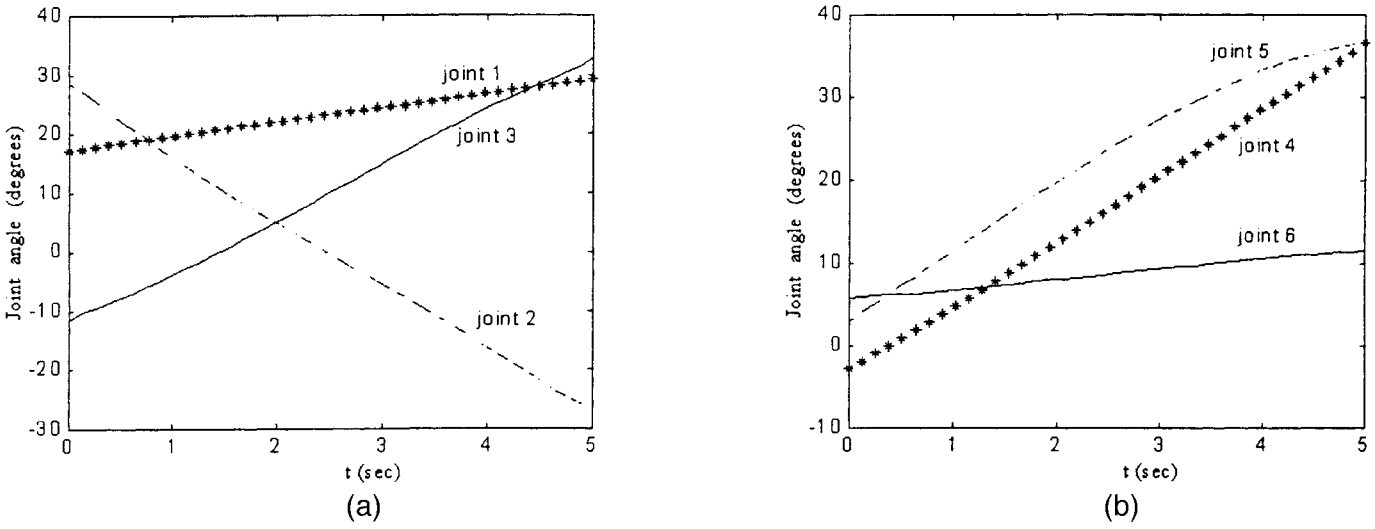


Fig. 6. Results for the designed optimum path of Fig. 4b in terms of time history of joint angle of: (a) joint 1 to 3; (b) joint 4 to 6 (angles are expressed in degrees).

occur to an object grasped by a two-finger gripper as pointed out in Ceccarelli.[18]

The static equilibrium of the grasped object can be expressed by using the model of Figure 3 along the directions of the contact and the squeezing lines in term of forces as

$$F_1 \cos\psi_1 - F_2 \cos\psi_2 + \mu_1 F_1 \sin\psi_1 - \mu_2 F_2 \sin\psi_2 + m_{object}(g \cos\psi_W \sin\Phi_W + a_y) = 0 \quad (33)$$

$$-F_1 \sin\psi_1 - F_2 \sin\psi_2 + \mu_1 F_1 \cos\psi_1 + \mu_2 F_2 \cos\psi_2 + m_{object}(g \cos\psi_W \cos\Phi_W + a_z) = 0 \quad (34)$$

and in term of torque as

$$r_A F_1(\sin\psi_1 - \mu_1 \cos\psi_1) - r_B F_2(\sin\psi_2 - \mu_2 \cos\psi_2) - N - r_G m_{object}(g + a_y) \sin\Phi_W = 0 \quad (35)$$

where the acceleration components a_y and a_z of the gravity center point on the manipulator extremity can be computed using Equation (12) as

$$\begin{bmatrix} a_x \\ a_y \\ a_z \\ 1 \end{bmatrix} = \left(\sum_{j=1}^{i} (U_{ij}\ddot{q}_j) + \sum_{j=1}^{i} (U_{ijk}\dot{q}_j\dot{q}_k) \right) \begin{bmatrix} r_{Gx} \\ r_{Gy} \\ r_{Gz} \\ 1 \end{bmatrix} \quad (36)$$

and r_G is the position vector of G.

Indeed, the directions of the friction forces, and consequently their sign in Equations (33) to (36) will be determined to be contrary to the relative motion object-finger when the static equilibrium has been computed.

Kinematic aspects of the grasp can be taken into account through ψ_1 and ψ_2, r_A, r_B and r_G. But, for the operation of the gripping mechanism they can be assumed as given and Equations (33) to (36) can be used to obtain the grasping

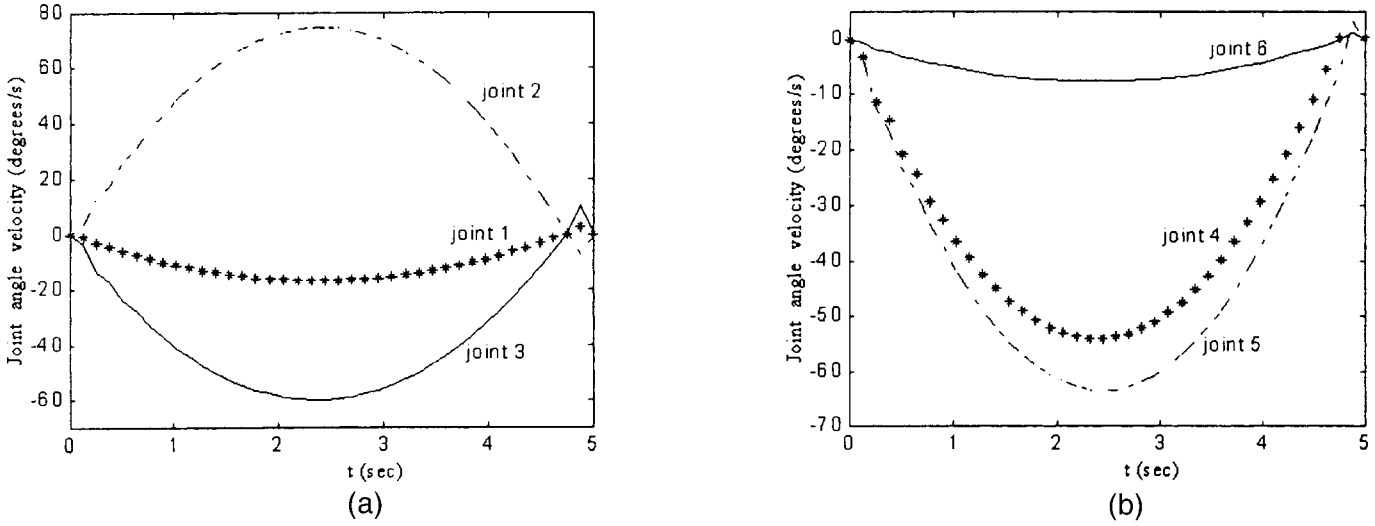


Fig. 7. Results for the designed optimum path of Fig. 4b in terms of time history of joint angle velocity of: (a) joint 1 to 3; (b) joint 4 to 6 (velocities are expressed in degrees/sec).

https://doi.org/10.1017/S0263574702004162 Published online by Cambridge University Press

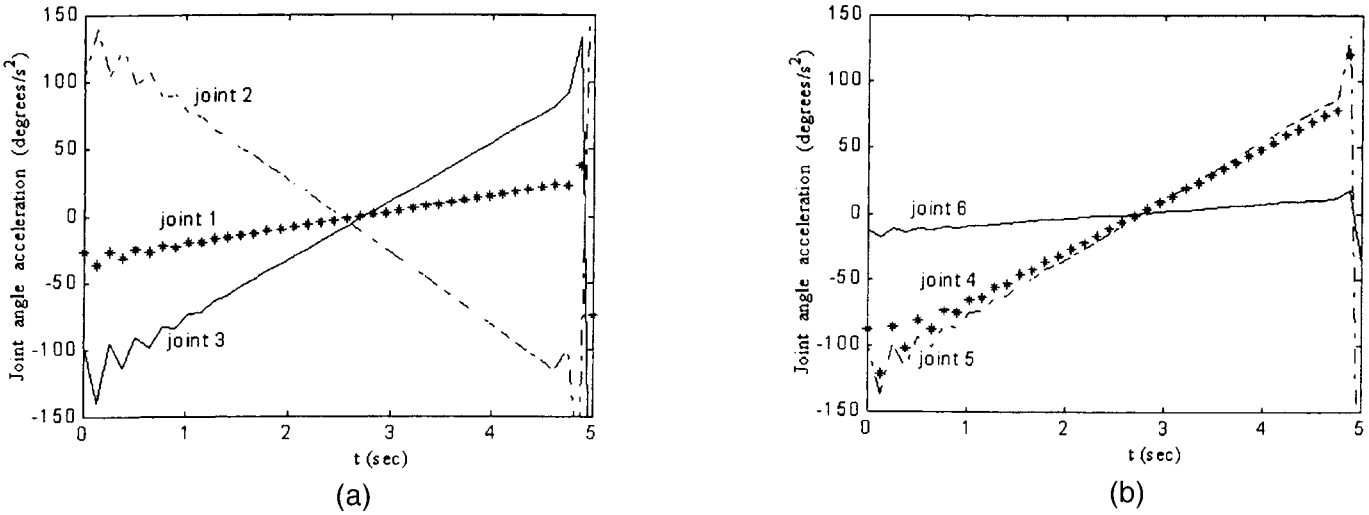


Fig. 8. Results for the designed optimum path of Fig. 4b in terms of time history of joint angle acceleration of: (a) joint I to 3; (b) joint 4 to 6 (accelerations are expressed in degrees/ sec^2).

forces F_1 and F_2 that are exerted by the gripping mechanism through the fingers.

6. A NUMERICAL EXAMPLE

A numerical example has been developed for a Puma 560 Robot[19] with six revolution joints. The illustrative manipulator task consists in transporting a payload from an initial point to a final one as shown in Figure 1. The Denavit-Hartenberg parameters are listed in Table I and the robot dynamics characteristics are given in Table II as deduced from references [15], [19]. The positions of centers of gravity are reported as r_x, r_y and r_z referring to the x, y and z coordinates of a center of gravity in the coordinate frame attached to the corresponding link. The diagonal terms of the inertia dyadics are represented by I_{xx}, I_{yy} and I_{zz} for each link, when the coordinate frame for the inertia dyadic terms is fixed at the center of gravity. The motor inertia terms are given by I_m. The limits for each i actuator in terms of maximum joint mobility Q_i, maximum velocity V_i, maximum acceleration W_i, and maximum torque Γ_i, and they are given in Table III as deduced from reference [19]. The payload constraints are expressed in terms of feasible range for the grasping forces given by $Fg_{min}=0$ and $Fg_{max}=60$ N. The grasped object mass is m=1.0 kg.

In the example, the robot is at rest initially and stops at the end of the trajectory. Thus, the initial and final velocities are zero for all joints. The trajectory time is adopted as $t_m=5.0$ sec. The initial and final trajectory points are given: $q_0=[0.30\ 0.50\ -0.20\ -0.05\ 0.05\ 0.10]$ and $q_m=[0.51\ -0.42\ 0.58\ 0.638\ 0.835\ 0.20]$ with angles expressed in radians. The path planning task has been described using m=40 knots in the trajectory of each joint of the manipulator.

The program DOT – Design Optimization Tools,[20] has been used for the sequential optimization method to solve the proposed optimization problem of Equations (1) and (2). A general analysis code has been developed in Fortran language by the authors by involving the dynamic model and trajectory planning of the robot as formulated in the

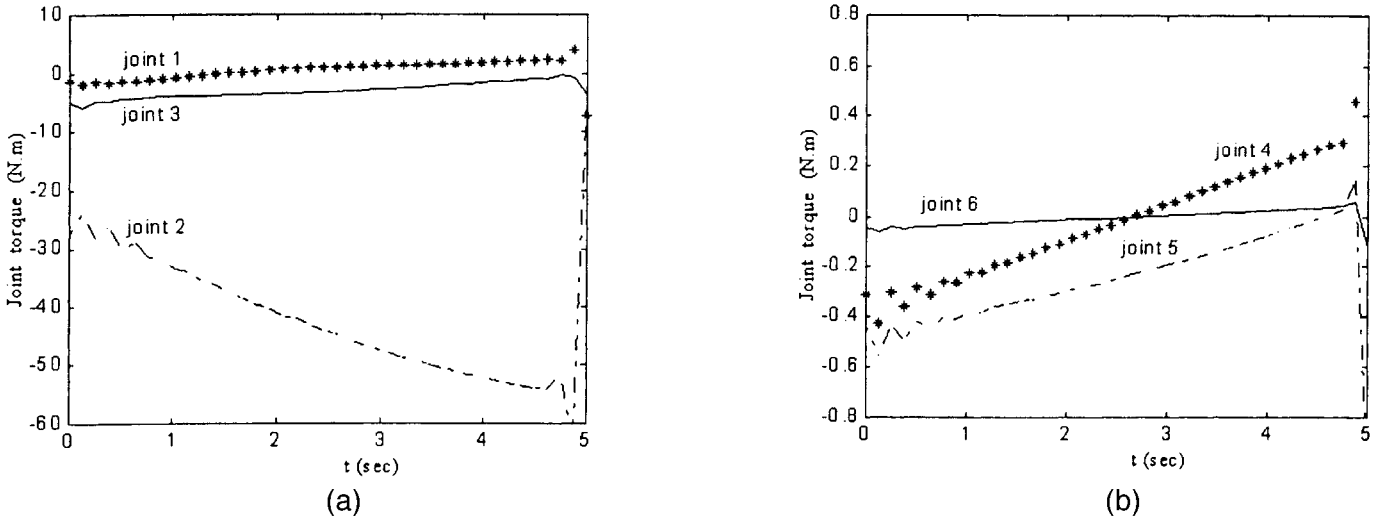


Fig. 9. Results for the designed optimum path of Fig. 4b in terms of time history of joint torque of: (a) joint 1 to 3; (b) joint 4 to 6 (torques are expressed in Nm).

https://doi.org/10.1017/S0263574702004162 Published online by Cambridge University Press

paper. DOT program and analysis code have been combined to solve numerically the proposed formulation for the optimum path planning with payload constraints by using Equations (1) to (36).

The prescribed manipulative task is shown in Figure 4a, and the obtained optimum path is traced in Figure 4b. Results for a numerical example of Figure 4 with data of Tables I, II, and III are shown in Figure 4 to 13. In particular, the guess path between the given points P_0 and P_m in Figure 4a) has been chosen as a straight line in the joint spaces, but the final optimized path of Figure 4b) is completely different as also shown by the Cartesian projections of Figure 5, which show a fairly smooth trajectory.

The excursions of the joint angles are significant and only joints 1 and 6 show a small motion as shown in Figure 6. At the end of motion some unexpected variations in velocity and mostly in acceleration are observable from Figures 7 and 9 for joints 2, 3, 4 and 5. They can be considered as due to numerical problems in solving the manipulator dynamics. and natural behavior of the manipulator, that because of its inertias can overshoot the final position. Numerical problems can be considered due both to the used numerical technique with its errors and the proposed model for the path planning with 40 knots for the B-splines and two additional conditions for the velocity constraints. Nevertheless, the obtained solution meets the prescribed condition of no velocity at the end point, although overshooting problems are observable mainly in the acceleration diagrams.

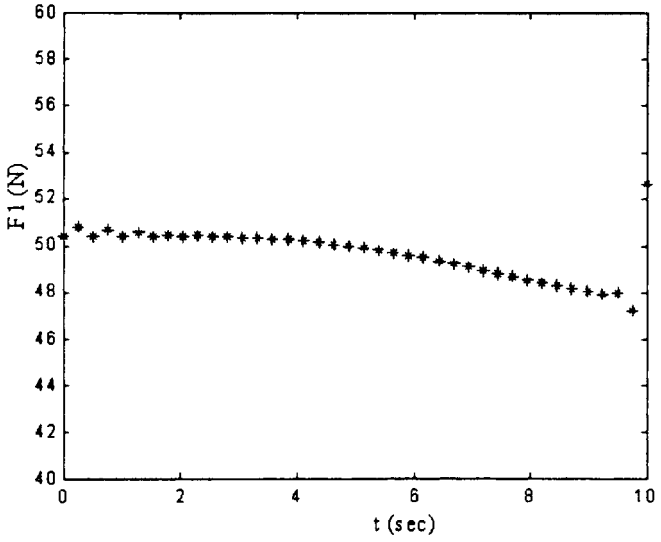


Fig. 10. Time history of the grasping force exerted by gripper finger during the designed optimum path of Fig. 4b (forces are expressed in N).

Figure 10 gives a significant result showing that the grasping force must be adapted smoothly to the manipulator dynamics in order to ensure the static equilibrium of the grasping.

Figure 11 shows the diagrams of the optimum B-splines as function of the knots and Figure 12 gives illustrative examples of the evolution in the computation of the optimum values during the optimization process. The peaks in the plots of Figure 12 are due to the search of the better optimum by updating all the variables and then the DOT algorithm changes one parameter at each step. The convergence to optimum values may be observed when the above mentioned updatings do not give larger variations in the spline coefficient variables.

Figure 13 shows the evolution of the objective function as a function of the number of the iteration steps of the DOT numerical technique. One can note and argue that the convergence is not evident and the minimum condition is not clearly met, although the numerical procedure has given the result as a feasible optimum solution. But the variation of mechanical energy is strongly constrained by physical constraints for the actuated joints and prescribed manipulative task so that the optimum solution can be considered as a combination of kinematical and dynamical optimum

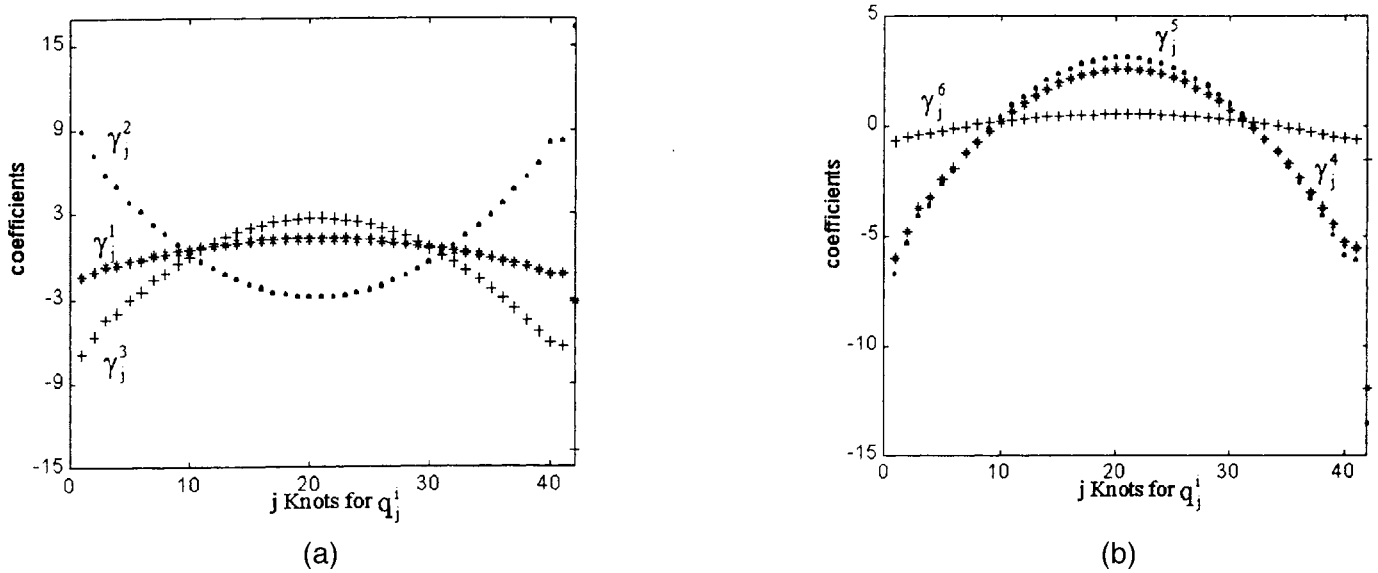


Fig. 11. Results for the designed optimum spline coefficients of: (a) joint 1 to 3; (b) joint 4 to 6 (the coefficients are expressed in degrees/s^3).

https://doi.org/10.1017/S0263574702004162 Published online by Cambridge University Press

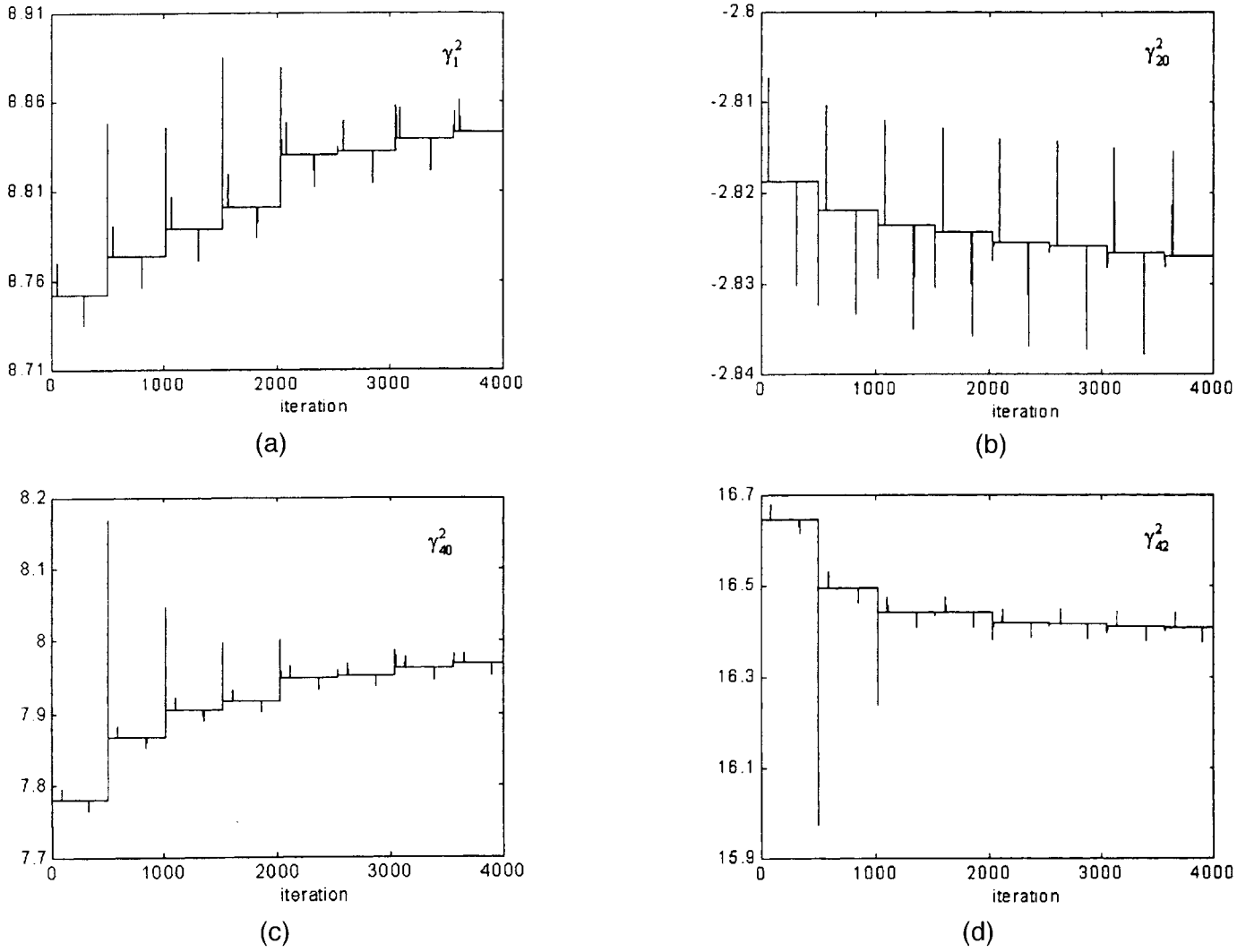


Fig. 12. Results for the some designed optimum spline coefficients of joint 2: (a) coefficient γ_1^2; (b) coefficient γ_{20}^2; (c) coefficient γ_{40}^2; (d) coefficient γ_{42}^2 (the coefficients are expressed in degress/s^3).

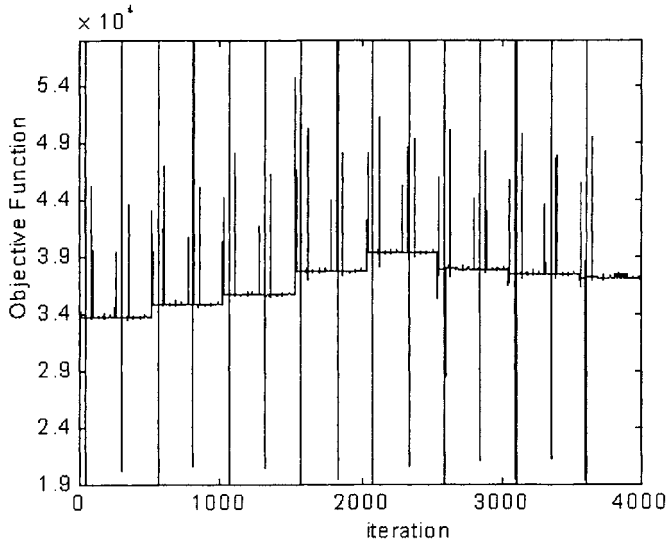


Fig. 13. Evolution of the optimum design for the numerical example of Fig. 4b in terms of objective function (the objective function is expressed in (Nm/s)^2).

characteristics, as those related to the joint movements. In fact, the obtained optimum path is characterized by suitable smooth joint trajectories, as shown in the diagrams of Figures 6, 7, 8 and 9, that are due to the corresponding smooth B-spline curves, as shown in Figure 11. In addition, the optimum solution for the energy consumption can be also characterized by the slight variation of the grasping force, as shown in Figure 10. In fact, the minimum of the energy consumption in the joints movement can be ensured by having minimum variations in both joint movements and joint torques, as indeed obtained from the diagrams of Figures 7 to 9.

7. CONCLUSIONS

This paper has presented a general formulation for the optimum path planning of robot manipulators of an industrial type, taking into account the grasping forces in the manipulator gripper. An optimization problem has been formulated by using the dynamics of Puma-like robots and statics of two-finger grasps. The joint trajectories have been written as cubic B-splines whose coefficients have been determined by using a *Fortran* code that has been

https://doi.org/10.1017/S0263574702004162 Published online by Cambridge University Press

specifically developed by the authors as combined with a numerical technique DOT code for solving optimization problems. The proposed formulation with a suitable numerical procedure for optimum path planning has been successfully applied to a Puma robot for a manipulator task of practical significance.

Acknowledgements

The first author is grateful to the Brazilian Ministry of Education (Capes) for the grant, which has permitted her to spend a sabbatical year in 2001 at the Laboratory of Robotics and Mechatronics in Cassino, Italy.

References

1. C.S. Lin, P.R. Chang and J.Y.S. Luh, "Formulation and Optimization of Cubic Polynomial Joint Trajectories for Industrial Robots", *IEEE Trans. Automat. Contr.* **28**, 1066–1073 (1983).
2. K.G. Shin and N.D. Mckay, "A Dynamic Programming Approach to Trajectory Planning of Robotic Manipulators", *IEEE Trans. Automat. Contr.* **AC-31**(6), 491–500 (1986).
3. Z. Shiller and S. Dubowsky, "Robot Path Planning with Obstacles, Actuator, Gripper, and Payload Constraints", *Int. J. Robotics Research* **8**(6), 3–18 (1989).
4. Y.C. Chen, "Solving Robot Trajectory Planning Problems with Uniform Cubic B-Splines", *Optimal Control Applications & Methods* **12**, 247–262 (1991).
5. S. Zeghloud, B. Blanchard and J.A. Pamanes, "Optimization of Kinematics Performances of Manipulators Under Specified Task Conditions", *Proceedings of the Tenth ClSM-lFToMM Symposium (Romansy 10)* Poland (1994) pp. 247–252.
6. D.P. Chevallier and S. Payandeh, "On Computation of Grasping Forces in Dynamic Manipulation Using a Three-Fingered Grasp", *Mechanism and Machine Theory* **33**(3), 225–244 (1998).
7. J. Zhao and S.X. Bai, "Load distribuition and joint trajectory planning of coordinated manipulation for two redundant robots", *Mechanism and Machine Theory* **34**, 1155–1170 (1999).
8. C.G. Johnson and D. Marsh, "Modelling robot manipulators with multivariate B-splines", *Robotica* **17**, Part 3, 239–247 (1999).
9. F.C. Park, J. Kim and J.E. Bobrow, "Algorithms for Dynamics-Based Robot Motion Optimization", *Tenth World Congress on the Theory of Machines and Mechanics (IFToMM)*, Finland (1999) pp. 1216–1221.
10. Y.K. Choi, J.H. Park, H.S. Kim and J.H. Kim, "Optimal trajectory planning and sliding mode control for robots using Evolution Strategy", *Robotica* **18**, Part, 423–428 (2000).
11. S. Arimoto, "Millenium Special Issue on Robotic Grasping and Manipulation", *Robotica* **18**, Part 1, 1–71 (2001).
12. M. Ceccarelli, F. Valero, V. Mata and I. Cuadrado, "Generation of adjacent configurations for a collision-free path planning of manipulators", *Robotica* **14**, Part, 391–396 (1996).
13. S.F.P. Saramago and V. Steffen Jr, "Optimal Trajectory Planning of Robot Manipulators in the Presence of Moving Obstacles", *Mechanism and Machine Theory* **35**(8), 1079–1094 (2000).
14. S.F.P. Saramago and V. Steffen Jr, "Optimization of the Trajectory Planning of Robot Manipulators taking into account the Dynamics of the System", *Mechanism and Machine Theory* **33**(7), 883–894 (1998).
15. B. Armstrong, O. Khatib and J. Burdick, "The Explicit Dynamic Model and Inertial Parameters of PUMA 560 Arm", *Proc. IEEE International Conference on Robotics and Automation*, San Francisco, California (April, 1986), **Vol. 1**, pp. 510–518.
16. S.F.P. Saramago and V. Steffen Jr, "Using B-Splines for Optimal Trajectory Planning"; *J. Sciences and Technology* **8**(1), 106–114 (1989).
17. M. Ceccarelli and N.J. Nieto, "El Agarre con Pinzas de Dos Dedos", *1° Congreso Iberoamericano de Ingenieria Mecanica*, Madrid (1993) **Vol. 4**, pp. 170–171.
18. M. Ceccarelli, "Design Problems for Industrial Robot Two-Finger Grippers", *3rd International Workshop on Robotics in Alpe-Adria Region RAA94*, Bled (1994), pp. 117–120.
19. Unimate® Industrial Robots, *Puma Mark III Robot 500 series for Val II – Operating Systems arm Equipament Manual*, Sections A1 to A6 (1986).
20. G. Vanderplaats, *DOT – Design Optimization Tools Program – Users Manual* (Vanderplaats Research & Development, Inc, Colorado Springs (1995).

https://doi.org/10.1017/S0263574702004162 Published online by Cambridge University Press